Macroscopic length changes due to the alignment of elastic dipoles in KCl

R. Balzer, H. Peters, and W. Waidelich

I. Physikalisches Institut der Technischen Hochschule Darmstadt, Darmstadt, Germany

H. Peisl

Physik-Department der Technischen Universität München, München, Germany

The creation of defects in a crystal leads to distortion of the lattice. Using the model of an elastic dipole for the defect the mechanical interaction of defects with the lattice can be described by double force tensors. Anisotropic defects as H and V_k centers in alkali halides lead to an anisotropic distortion of the crystal. These defects are created in different (equivalent) orientations inducing an isotropic (macroscopic) length change. This equivalent distribution of defects can be disturbed by irradiation with polarized light, thus turning defects from one orientation to another. This results in a change of the macroscopic dimensions of the crystal and the length change in different directions of the crystal is a measure for the anisotropy of the distortion field induced by the defect. If a sufficient amount of anisotropic defects can be turned from one orientation into another, the corresponding macroscopic length change can be measured in different directions. In addition, the concentration of the turned defects is measured via optical-absorption measurements and the double force tensor for the H and the V_k center in KCl is determined.

I. INTRODUCTION

The creation of lattice defects leads to a change of most of the macroscopic features of the crystal. Defects in the alkali halides, especially, give rise to characteristic absorption bands in the otherwise transparent range between about 0.1 and 6 eV. Via optical-absorption measurements, information about the various defects and their concentrations can be obtained very easily. In general, defects also have a strong elastic interaction with the host lattice. This gives rise to a distortion of the host lattice. The distortion of the lattice can be described by a force array which would cause the same distortion in a perfect lattice. The dipole part of the force distribution, which is called elastic dipole, describes the long-range part of the distortion field and the macroscopic volume change of the crystal.[1-3] H and V_k centers in alkali halides are optically and mechanically anisotropic. Both centers are well known from ESR and optical measurements. The H center can be described as a Cl_2^- molecule on *one* lattice site or, more generally, as an interstitial atom. The V_k center is a Cl_2^- molecule on *two* lattice sites and represents a trapped-hole center. Both centers involve an anisotropic distortion of the crystal. The optical and the elastic dipole axes are along $\langle 110 \rangle$ directions. Due to the high symmetry of the cubic lattice there exist six equivalent orientations for $\langle 110 \rangle$ oriented defects. These orientations usually are equally populated. An experimentally induced change of the population in different orientations allows one to measure the components of the elastic dipole tensor. If uniaxial stress is applied to the crystal, the orientationally degenerate levels split. The population of the now-energetically-different levels obeys a Boltzmann distribution. The concentration of the defects of different orientations as a function of applied stress can be measured by optical absorption. This gives information about the anisotropic part of the double force tensor describing the elastic dipoles.[1]

A new method to determine the elastic dipole tensor will be described here.[4] It takes advantage of the possibility to rotate anisotropic defects by polarized light. The anisotropic defects considered here have a well-defined reorientation temperature. Above this temperature, defects will reorientate until all orientations in the crystal are equally occupied. Below this temperature (10.9 K for H centers in KCl), defects can be rotated only via their excited state, i.e., by illumination with light of the wavelength of the absorption band of this center. If this light is polarized, only defects with their transition dipole moment not perpendicular to the electric vector of the incident light can be rotated. After excitation the orientation of the defects will be distributed statistically over the six possible orientations. Thus the orientation of the dipoles that were excited will be depopulated, and it is possible to bring defects from one orientation to another.

Rotation of an anisotropic defect involves rotation of the defect-induced strain field, which causes measurable macroscopic length change of the crystal. Optical-absorption measurements with polarized light give information about the defect concentration in the different orientations.
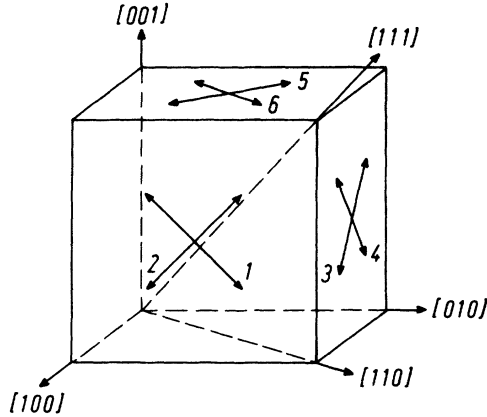
FIG. 1. The six possible orientations of a $\langle 110 \rangle$-oriented defect in a cubic lattice.

At least three sets of measurements in different directions of the crystal are necessary to calculate the double force tensor for the H and the V_k center.

II. LATTICE DISTORTION DUE TO ELASTIC DIPOLES

H and V_k centers are both oriented along $\langle 110 \rangle$ axes. Figure 1 shows the six possible orientations in the cubic lattice. All orientations are usually equally occupied. Bleaching or application of external stress will change the population in the different orientations and for detailed discussions it is necessary therefore to distinguish between the possible orientations. For the following calculations the notation 1–6 for the different defect orientations is used, as shown in Fig. 1. Figure 2 shows the well-known models of an H and a V_k center; ξ, η, ζ are the coordinates along the main axes of the defect, and x, y, z are the crystal coordinates.

The model of an elastic dipole can be used to describe the elastic interaction of an anisotropic defect. The interaction energy of an elastic dipole with an external strain field is defined as

$$U = - \overset{\leftrightarrow}{\mathbf{P}} \cdot \overset{\leftrightarrow}{\epsilon}, \tag{1}$$

in analogy to the electric dipole, which interacts with an electric field. $\overset{\leftrightarrow}{\mathbf{P}}$ is the double force tensor characterizing the elastic dipole, and $\overset{\leftrightarrow}{\epsilon}$ describes the external strain field in continuum approximation. The double force tensor describes the defect-induced stress around the defect, and has the same symmetry and the same transformation behavior as the distortion tensor.

The H and V_k centers in a fcc lattice are of orthorhombic symmetry. In principal axes, the double force tensor $\overset{\leftrightarrow}{\mathbf{P}}$ can be written as

$$\overset{\leftrightarrow}{\mathbf{P}} = \begin{pmatrix} P_{\xi\xi} & 0 & 0 \\ 0 & P_{\eta\eta} & 0 \\ 0 & 0 & P_{\zeta\zeta} \end{pmatrix} . \tag{2}$$

The transformation to crystal coordinates leads to

$$\overset{\leftrightarrow}{\mathbf{P}} = \begin{pmatrix} P_{xx} & P_{xy} & 0 \\ P_{xy} & P_{xx} & 0 \\ 0 & 0 & P_{zz} \end{pmatrix} , \tag{3}$$

with

$$P_{xx} = \tfrac{1}{2}(P_{\xi\xi} + P_{\zeta\zeta}),$$
$$P_{xy} = \tfrac{1}{2}(P_{\xi\xi} - P_{\zeta\zeta}), \tag{4}$$
$$P_{zz} = P_{\eta\eta} .$$

The distortion in a cubic lattice due to a [110]-oriented orthorhombic defect can be written as

$$\overset{\leftrightarrow}{\epsilon} = \begin{pmatrix} \epsilon_{xx} & \epsilon_{xy} & 0 \\ \epsilon_{xy} & \epsilon_{xx} & 0 \\ 0 & 0 & \epsilon_{zz} \end{pmatrix} , \tag{5}$$

with

$$\epsilon_{xx} = \tfrac{1}{2}(\epsilon_{\xi\xi} + \epsilon_{\zeta\zeta}),$$
$$\epsilon_{xy} = - \tfrac{1}{2}(\epsilon_{\xi\xi} - \epsilon_{\zeta\zeta}), \tag{6}$$
$$\epsilon_{zz} = \epsilon_{\eta\eta} ,$$

$\epsilon_{\xi\xi}, \epsilon_{\eta\eta}, \epsilon_{\zeta\zeta}$ being the strain components along the main axes of the defect, induced by one defect and normalized to one atomic volume. Application of Hooke's law gives the connection with the double force tensor
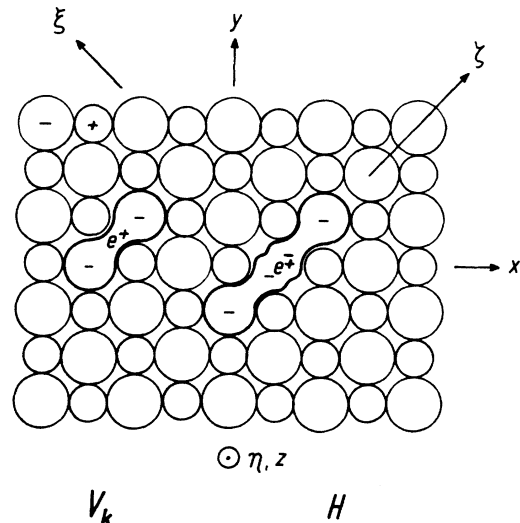

FIG. 2. H and V_k centers in alkali halides.

$$\epsilon_{xx} = \frac{1}{(a/2)^3} [S_{11} P_{xx} + S_{12}(P_{xx} + P_{zz})],$$

$$\epsilon_{zz} = \frac{1}{(a/2)^3} (S_{11} P_{zz} + 2S_{12} P_{xx}), \tag{7}$$

$$\epsilon_{xy} = \frac{1}{2(a/2)^3} S_{44} P_{xy},$$

with S_{ik} being the elastic compliance constants of the crystal along its main axes, and $(a/2)^3$ being the atomic volume. The macroscopic length

change in one crystal direction, owing to reorientation of anisotropic defects, is now obtained as a projection of all distortion components along this direction multiplied by the corresponding change of the defect concentration.

Length-change measurements along the [001], [110], and [111] directions are sufficient to determine all components of the double force tensor of the defect. The defect-induced length changes are described:

(a) length change parallel to [001],

$$\left(\frac{\Delta l}{l}\right)_{001} = \epsilon_{xx} \Delta c_{1-4} + \epsilon_{zz} \Delta c_{56}$$

$$= \frac{1}{(a/2)^3} \{[S_{11} P_{xx} + S_{12}(P_{xx} + P_{zz})] \Delta c_{1-4} + (S_{11} P_{zz} + 2S_{12} P_{xx}) \Delta c_{56}\}; \tag{8}$$

(b) length change parallel to [110],

$$\left(\frac{\Delta l}{l}\right)_{110} = \tfrac{1}{2}(\epsilon_{xx} + \epsilon_{zz})\Delta c_{1-4} + \epsilon_{xx}(\Delta c_5 + \Delta c_6) - \epsilon_{xy}(\Delta c_5 - \Delta c_6)$$

$$= \frac{1}{(a/2)^3} \left[\left(\frac{S_{11} + 3S_{12}}{2} P_{xx} + \frac{S_{11} + S_{12}}{2} P_{zz}\right) \Delta c_{1-4} + [S_{11} P_{xx} + S_{12}(P_{xx} + P_{zz})](\Delta c_5 + \Delta c_6) - \tfrac{1}{2}S_{44} P_{xy}(\Delta c_5 - \Delta c_6)\right]; \tag{9}$$

(c) length change parallel to [111],

$$\left(\frac{\Delta l}{l}\right)_{111} = (\tfrac{2}{3}\epsilon_{\zeta\zeta} + \tfrac{1}{3}\epsilon_{\eta\eta})\Delta c_{135} + (\tfrac{2}{3}\epsilon_{\zeta\zeta} + \tfrac{1}{3}\epsilon_{\eta\eta})\Delta c_{246}$$

$$= \frac{1}{(a/2)^3}\{ [\tfrac{2}{3}(S_{11} + 2S_{12})P_{xx} + \tfrac{1}{2}P_{zz} - \tfrac{1}{3}S_{44} P_{xy}]\Delta c_{135} + [\tfrac{2}{3}(S_{11} + 2S_{12})(P_{xx} + \tfrac{1}{2}P_{zz}) + \tfrac{1}{3}S_{44} P_{xy}]\Delta c_{246}\}. \tag{10}$$

Δc_i is the change of defect concentration in the ith orientation.

$$c_{1-4} = c_1 + c_2 + c_3 + c_4,$$

$$c_{56} = c_5 + c_6,$$

$$c_{246} = c_2 + c_4 + c_6,$$

$$c_{135} = c_1 + c_3 + c_5.$$

III. OPTICAL FEATURES OF H AND V_k CENTERS

The allowed optical transitions of Cl_2^- molecule centers were derived in analogy to the spectrum of the free Cl_2 molecule. The strongest optical transition of the free molecule as well as the Cl_2^- centers are in the near uv and are strongly σ polarized.

Light with its electric vector perpendicular to the center axis—i.e., π polarized—is only weakly absorbed and will be neglected in the following discussions.[5-7] The defect concentrations contributing to the optical absorption can be obtained from Smakula equation,

$$nf = (\text{const})k_{max} H, \tag{11}$$

where n is the number of centers per unit volume,

k_{max} is the absorption coefficient at the band maximum, H is the half-width of the absorption band, and f is the oscillator strength.

The oscillator strength f is usually defined for absorption with unpolarized light. For anisotropic defects it is necessary to define oscillator strengths in all three different possible polarizations. There are f_σ for the $\langle 110 \rangle$ or molecule axis, f_{r_1} and f_{r_2} for the two directions perpendicular to the molecule axis.[8] With f_σ large compared to f_{r_1} and f_{r_2}, one obtains

$$f = \tfrac{1}{3}(f_\sigma + f_{r_1} + f_{r_2}) \simeq \tfrac{1}{3}f_\sigma. \tag{12}$$

The value of f is independent of the polarization direction of the incident light. If the centers are not equally distributed over the different orientations, this equation is not valid any more. The different orientations give different contributions to the absorption. One obtains

$$k_{max}^{hkl} = \frac{N}{(\text{const})H} \sum_{i=1}^{6} c_i f_i^{hkl}, \tag{13}$$

c_i being the defect concentration in the different orientations and

$$f_i^{hkl} = f_\sigma \cos^2 \alpha_i,$$

TABLE I. Oscillator strengths f_i^{hkl} along the directions [001], [110], and [111] for the six possible orientations of the oscillator. Notation i is according to Fig. 1.

i	f_i^{001}	f_i^{110}	f_i^{111}
	f_σ	f_σ	f_σ
1	1/2	1/4	0
2	1/2	1/4	2/3
3	1/2	1/4	0
4	1/2	1/4	2/3
5	0	0	0
6	0	1	2/3

with α_i the angle between the direction of the electric vector of the analyzer light and the main axis of the defect. Table I gives the values f_i^{hkl} for three different experimentally interesting directions. For equally distributed defects, Eq. (13) can be replaced again by Eqs. (11) and (12).

IV. EXPERIMENTAL PROCEDURE AND RESULTS

The experimental method described here is based on the combined measurement of the macroscopic length and the optical absorption of the crystal. Optical-absorption measurements with polarized light give information about the defect concentration in the different orientations. Rotation of the anisotropic defect by illumination with polarized light involves rotation of the defect-induced strain field, which causes measurable macroscopic length change of the crystal. This experiment can be done in different directions of the crystal and the double force tensor, describing the elastic interaction of the defect with the lattice thus can be obtained. Figure 3 shows the experimental setup for such an experiment. For length-change measurements an inductive transducer is used with an accuracy of $(\Delta l/l) = 5 \times 10^{-7}$. This inductive transducer is mounted inside the cryostat to avoid any error due to long transmission rods. The analyzer light hits the crystal perpendicular to the direction where the length change of the
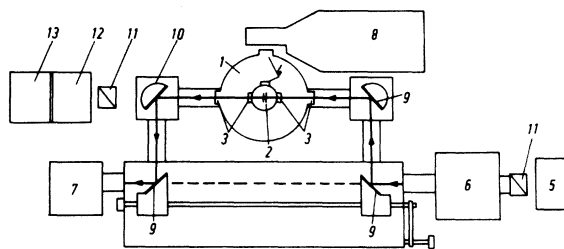

FIG. 3. Experimental setup. 1, cryostat; 2, crystal; 3, optical window; 4, x-ray window; 5–7, spectrometer; 8, x-ray tube; 9 and 10, mirror; 11, polarizer; 12 and 13, light source for bleach.

crystal is measured, and the polarization of the analyzer light is either parallel to the direction of the length-change measurement or perpendicular. One of the mirrors can be taken off and put in again, highly reproducible in order to do the bleaching with a light source much stronger than that of the analyzer. The defects are created initially at 6 K by irradiation with a 150-kV x-ray tube, usually operated at 100 kV, 18 mA. Figure 4 shows a typical absorption spectrum. The solid curve shows the absorption for equally distributed defects right after x irradiation. Measurements with [001] and [010] polarized light give the same absorption. Subsequent illumination with light polarized along [001] depopulates all orientations except those perpendicular to the [001] direction. Thus the absorption polarized along [001] decreases, whereas the absorption polarized along [010] grows. This is shown in the curves (a) and (b) of Fig. 4.

Figure 5 shows the results for one direction. The relative length change is measured in the [001] direction, and the optical-absorption measurement is done for [001] and [010] polarization. The cubes below the drawings show schematically the experimental procedure.

The experiment starts with the irradiated crystal; the defects are equally distributed over the different orientations. Now the crystal is bleached in the [100] direction with the light polarized in the [001] direction. The concentration of all defects that are not perpendicular to the electric vector of the bleach light decreases, and the concentration of the defects in orientations perpendicular to the electric vector grows. After completion of this bleach, the concentration in four orientations is reduced by approximately 50%. These orientations are no longer shown on the schematic, although they are not completely bleached out.
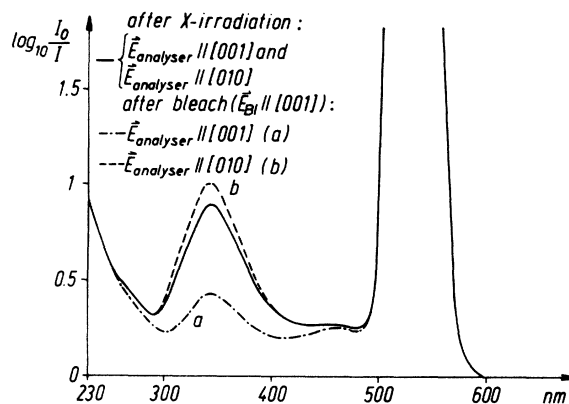

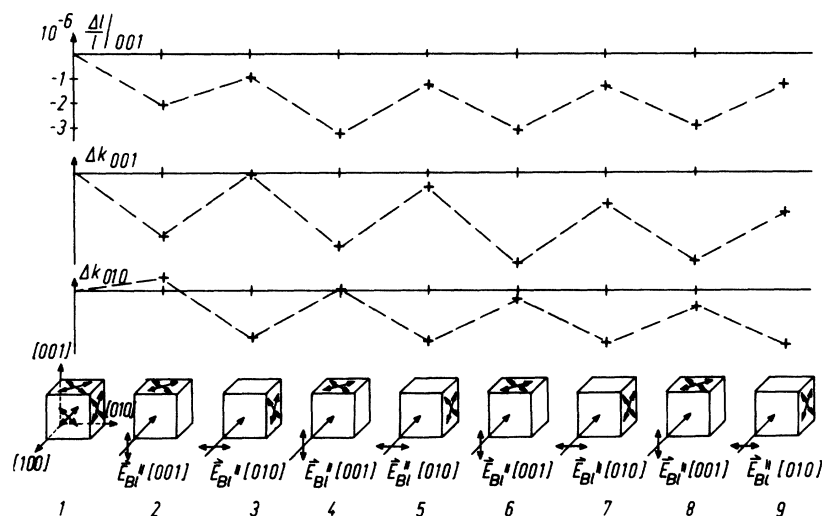FIG. 4. Absorption spectrum of KCl after x irradiation at 8 K.

FIG. 5. Relative length change, [001], and [010] polarized optical absorption (345 nm) after bleach of H and V_k centers with [001] and [010] polarized light, respectively.

Now the first data points are taken. The total length of the crystal has decreased in the [001] direction; that means the defects in the new orientation induce less dilatation in this direction. For the next bleach, the polarization is turned by 90°, which leads to a reorientation of the defects from the (001) plane to the (010) plane, as shown in the schematic. This procedure can be repeated periodically and is shown here for eight successive steps.

Figure 6 shows the results for another measurement. The crystal is cut and oriented for relative length-change measurements in the [110] direction. Bleaching and optical-absorption measurements are done in the [110] and [001] direc-

tion. The schematic at the bottom again demonstrates the procedure: The experiment starts with an equal distribution of the anisotropic defects over the six possible orientations. Bleaching with [001] polarized light in the [110] direction depopulates the orientations in (100) and (010). Then the crystal is bleached with [110] polarized light. This leads to a saturation for defects with dipole axis along [110] and all other orientations are depopulated. Subsequent change of polarization of the bleach light does not give any change of this stabilized situation. This is verified for the length-change measurements as well as for the optical-absorption measurements. Only a small change can be noticed for the last three sets of data points. H and V_k centers together contribute to the optical-absorption band which peaks at approximately 345 nm. One of the main difficulties in this experiment results in the strong overlap of the two absorption bands of the H and
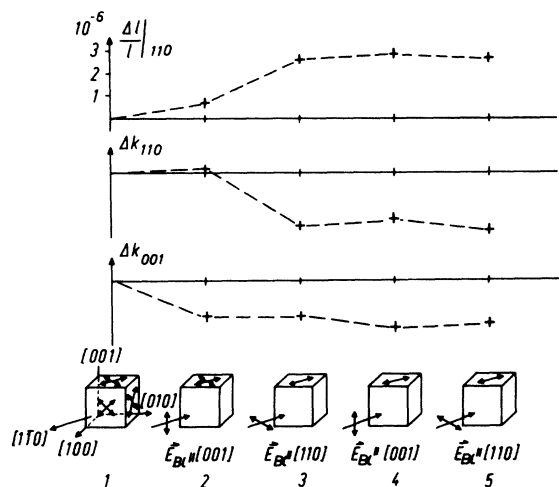

FIG. 6. Relative length change, [001], and [110] polarized optical absorption (345 nm) after bleach of H and V_k centers with [001] and [110] polarized light, respectively.
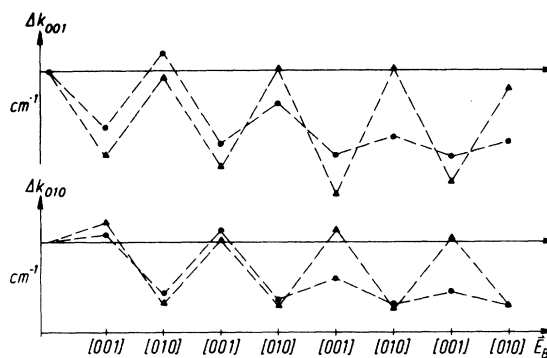

FIG. 7. Absorption constant of H centers (▲) and V_k centers (●) after successive steps of bleaching with [001] and [010] light.

TABLE II. Constants used to analyze the optical-absorption data of this experiment.

Absorption band	λ(nm)	E(eV)	H (eV)	f	f_σ
F	535	2.32	0.169	0.53	
H	336	3.69	0.66		0.90
V_k	365	3.40	0.81		0.48

the V_k center, which are located at 335 nm for the H band and at 365 nm for the V_k band. The two bands can be separated, assuming that the H band as well as the V_k absorption band are of Gaussian shape[9]:

$$k_H = k_{H\,max} + k_{V_k\,max} \exp\left[-0.692\left(\frac{2(E_H - E_{V_k})}{H_{V_k}}\right)^2\right],$$

TABLE III. Length change and optical absorption of F, H, and V_k centers due to optical reorientation of H and V_k centers.

(a) Length-change measurements along [001]

Crystal No.	Polarization of bleach light	Δk^H_{001} (cm^{-1})	Δk^H_{010} (cm^{-1})	$\Delta k^{V_k}_{001}$ (cm^{-1})	$\Delta k^{V_k}_{010}$ (cm^{-1})	Δk^F (cm^{-1})	$(\Delta l/l)_{001}$ (10^{-6})
1	001	−4.45	+1.05	−2.96	+0.37	−9.80	−2.10
	010	+4.13	−4.13	+3.90	−3.14	−4.13	+1.11
	001	−4.73	+3.35	−4.76	+3.34	−8.83	−2.40
	010	+5.17	−3.43	+2.12	−3.63	−3.31	+2.16
	001	−6.40	+4.03	−2.71	+1.13	−12.14	−1.89
	010	+6.40	−4.22	+0.94	−1.38	−1.10	+1.83
	001	−5.97	+3.78	−1.03	+0.62	−4.01	−1.53
	010	+4.90	−3.69	+0.79	−0.72	−0.69	+1.53
2	001	−9.39	+1.76	−4.13	+0.04	−12.00	−2.64
	010	+4.39	−1.45	+0.73	−0.57	−6.62	+1.58
3	010	+.150	−2.04	+1.26	−2.27	−10.35	+0.50
	001	−8.29	+4.39	−7.05	+1.55	−10.22	−3.71
	010	+8.09	−5.06	+2.41	−3.13	−3.73	+3.53
	001	−9.06	+4.20	−4.10	+0.57	−4.01	−4.00

Crystal No.	Polarization of bleach light	Δk^H_{001} (cm^{-1})	Δk^H_{110} (cm^{-1})	$\Delta k^{V_k}_{001}$ (cm^{-1})	$\Delta k^{V_k}_{110}$ (cm^{-1})		
4	001	−6.87	+0.41	−2.72	−1.75	−5.80	−1.57
	110	+2.16	−4.25	−0.37	−1.42	−12.14	+0.50
	001	−2.41	−0.67	−2.37	−0.26	−8.42	−0.69
	110	−0.55	−1.99	+1.84	−0.80	−2.62	+0.12

(b) Length-change measurements along [110]

Crystal No.	Polarization of bleach light	Δk^H_{110} (cm^{-1})	Δk^H_{001} (cm^{-1})	$\Delta k^{V_k}_{110}$ (cm^{-1})	$\Delta k^{V_k}_{001}$ (cm^{-1})	Δk^F (cm^{-1})	$(\Delta l/l)_{110}$ (10^{-6})
5	001	+0.69	−3.66	+0.15	−3.19	−8.83	+0.61
	110	−6.94	−1.49	−5.19	−1.34	−18.35	+1.30
	001	+.73	−0.77	+0.54	−0.78	−4.00	+0.26
	110	−0.60	+0.12	+1.02	+0.06	−7.04	−0.17
6	110	−8.49	−5.79	−4.65	−3.33	−21.66	+1.99
	001	+1.45	−1.42	0	−1.57	−5.38	+0.38

(c) Length-change measurements along [111]

Polarization of bleach light	Δk^H_{111} (cm^{-1})	Δk^H_{011} (cm^{-1})	$\Delta k^{V_k}_{111}$ (cm^{-1})	$\Delta k^{V_k}_{011}$ (cm^{-1})	Δk_F (cm^{-1})	$(\Delta l/l)_{111}$ (10^{-6})
111	−6.94	−3.45	−2.57	−1.56	−13.24	+0.42
011	+5.51	−3.47	+1.50	−5.97	−4.14	−0.70
111	−4.84	+9.34	−2.08	−0.16	−5.52	+0.84
011	+3.97	−11.94	+1.74	−0.58	−9.53	−0.60
111	−3.88	+4.92	−2.06	+5.20	−7.32	+0.65
111	−3.05	+4.76	−0.23	+1.30	−8.00	+0.60
111	−0.47	−0.20	−0.09	+0.49	−1.10	+0.12

TABLE IV. Relative length change and optical absorption of F, H, and V_k centers due to F-light bleach.

Crystal No.	k_H	k_{V_k}	k_F	$\Delta l/l$
	(cm^{-1})	(cm^{-1})	(cm^{-1})	(10^{-6})
8	7.40	5.46	101.7	
				0 ± 0.10 F bleach
	6.87	2.99	64.1	
				-0.04 ± 0.04 F bleach
	6.56	2.63	57.4	
				warm up to 40 K
	7.05	1.70	47.9	
				0 ± 0.12 F bleach
	6.77	1.61	45.7	

$$k_{V_k} = k_{H\,\text{max}} \exp\left[-0.692\left(\frac{2(E_H - E_{V_k})}{H_H}\right)^2\right] + k_{V_k\,\text{max}},$$

(14)

with E_i the energy at the maximum of the absorption band i. k_i is the absorption coefficient at the maximum of the absorption band i obtained from the 345-nm band, and $k_{i\,\text{max}}$ is the absorption coefficient of the band i.

Figure 7 shows the absorption separated for H and V_k centers for a typical experiment. Whereas the H centers can be reoriented without noticeable annealing, the V_k-center concentration decreases rapidly during successive steps of bleaching. To be able to correct for possible length changes induced by defect annealing the F-center concentration has been controlled for all measurements.

Table II gives the values used to calculate the defect concentrations from optical-absorption measurements for F, H, and V_k centers in KCl. Table III gives the results for seven crystals with length-change measurements in the [100], [110], and [111] directions. Table IV shows the results for another experiment which studies the annealing behavior of the irradiation-induced defects due to bleaching with F light.

V. DISCUSSION

With the results given in Table III and Eqs. (8)–(10), it is possible to evaluate the double force tensor for the H center as well as the V_k center. As an example, Fig. 8 shows the evaluation of the length-change measurements parallel to [001] and subsequent optical bleaching with light polarized along [001] and [010], respectively. The length change is plotted versus the concentration change Δc_{1-4}, and the slope of the so-obtained line directly gives $P_{xx} - P_{zz}$ for the H center in KCl. During reorientation processes also, defect recombination takes place. Irradiation-induced defects are produced as Frenkel pairs and recombination takes place via Frenkel-pair recom-

bination. H and F centers recombine leading to the undisturbed lattice, and V_k and F center recombination leads to the creation of an α center. To make the proper correction for the annealing to Eqs. (8)–(10), the following term must be added:

$$\left(\frac{\Delta l}{l}\right)_{\text{ann}} = \frac{1}{3}\left(\frac{\Delta v}{v}\right)_F \Delta c_{H\,\text{ann}} + \frac{1}{3}\left[\left(\frac{\Delta v}{v}\right)_\Gamma - \left(\frac{\Delta v}{v}\right)_\alpha\right]\Delta c_{V_k\,\text{ann}},$$

(15)

with $\Delta c_{H\,\text{ann}} + \Delta c_{V_k\,\text{ann}} = \Delta c_F$.

As could be shown in Fig. 7 the H-band absorption change due to annealing is negligible compared to the annealing rate of the V_k centers, so that

$$\Delta c_{H\,\text{ann}} \simeq 0, \quad \Delta c_{V_k\,\text{ann}} \simeq \Delta c_F .$$

To be able to correct for the V_k-center annealing, a separate experiment has been made. The annealing behavior of irradiation-induced defects due to F-band bleaching has been studied (Table IV).

The recombination-induced length change due to F-light bleach can be written

$$\frac{\Delta l}{l} = \frac{1}{3}\left[\left(\frac{\Delta v}{v}\right)_F + \left(\frac{\Delta v}{v}\right)_H\right]\Delta c_H$$
$$+ \frac{1}{3}\left[\left(\frac{\Delta v}{v}\right)_F + \left(\frac{\Delta v}{v}\right)_{V_k} - \left(\frac{\Delta v}{v}\right)_\alpha\right]\Delta c_{V_k} . \quad (16)$$

With the known values[10-12] $(\Delta v/v)_F = 0.6$, $(\Delta v/v)_H = 0.6$, and $(\Delta v/v)_\alpha = 0.7$ for KBr and $(\Delta v/v)_F = 0.6$ for KCl, $(\Delta v/v)_H$ and $(\Delta v/v)_\alpha$ were assumed to be of the same order of magnitude for KCl and KBr. With this assumption the volume change of a V_k center was obtained with the results of Table IV, using Eq. (16) to be $(\Delta v/v)_{V_k} = 0 \pm 0.1$. This result corresponds well with the description of the V_k center in KCl as a small polaron.[13] Although ENDOR measurements[14] show great displacements of the next neighbors around the defect, the long-range lattice distortions measured as macroscopic length changes are very small. As a result the double force tensors for the H and the V_k center are obtained in defect coordinates.
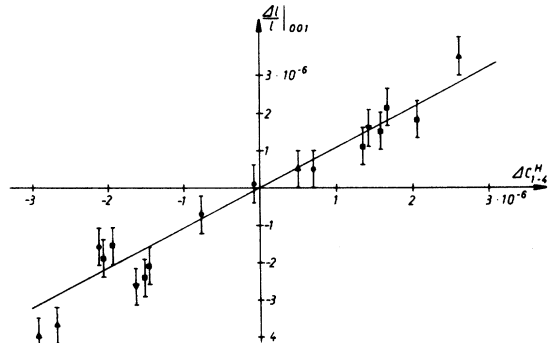

FIG. 8. Determination of $P_{xx}^H - P_{zz}^H$.

Double force tensor for an H center in KCl,

$$\overline{\overline{p}}^H = \begin{pmatrix} 6.3 & 0 & 0 \\ 0 & -3.7 & 0 \\ 0 & 0 & 4.3 \end{pmatrix} (eV) ;$$

double force tensor for a V_k center in KCl,

$$\overline{\overline{p}}^{V_k} = \begin{pmatrix} 0.6 & 0 & 0 \\ 0 & -0.9 & 0 \\ 0 & 0 & 0.3 \end{pmatrix} (eV) .$$

Bachmann and Känzig[1] measured the anisotropic part of the double force tensor of the H center,

$$\overline{\overline{P}}'^H = \overline{\overline{P}}^H - \tfrac{1}{3} Tr \overline{\overline{P}}^H ,$$

in KCl with a different method. They applied uniaxial stress to the crystal and measured the change of the population of the now-energetically-different levels. They obtained $P'^H_{\ell\ell} = 3.0$ eV $P'^H_{mm} = -5.2$ eV, and $P'^H_{\zeta\zeta} = 2.2$ eV. Using $Tr P^H = 6.9$ eV, this is in quite good agreement with our results.

[1]K. Bachmann and W. Känzig, Phys. Kondens. Mater. 7, 284 (1968).

[2]E. Kröner, Ergeb. Angew. Math 5, 1 (1958).

[3]R. T. Shuey and H. U. Beyeler, Z. Angew. Math. Phys. 19, 278 (1968).

[4]H. Peisl, R. Balzer, and H. Peters, Phys. Lett. A 46, 263 (1973).

[5]W. D. Compton and C. C. Klick, Phys. Rev. 110, 340 (1958).

[6]C. J. Delbecq, B. Smaller, and P. H. Yuster, Phys. Rev. 111, 1235 (1958).

[7]C. J. Delbecq, W. Hayes, and P. H. Yuster, Phys.

Rev. 121, 1043 (1961).

[8]D. York le Corgne, dissertation (University of Illinois, Urbana, 1970) (unpublished).

[9]H. Peisl, Z. Angew. Phys. 14, 529 (1962).

[10]R. Balzer, H. Peisl and W. Waidelich, Z. Phys. 204, 405 (1967).

[11]B. von Guérard, H. Peisl, and W. Waidelich, Z. Phys. 220, 473 (1969).

[12]R. Balzer, Z. Phys. 234, 242 (1970).

[13]J. Appel, Phys. Status Solidi 21, 193 (1968).

[14]D. F. Daly and R. L. Mieher, Phys. Rev. 183, 368 (1969).